Inorg. Chem. **2002**, *41*, 892–900

DFT Analysis of the Activation and Breaking of the Mo–N Bond in a (μ-Nitrido)dimolybdenum Complex: Is Molybdenum Tris(thiolate) an Elusive Intermediate?

Marie-Madeleine Rohmer and Marc Bénard*

Laboratoire de Chimie Quantique, UMR 7551, CNRS and Université Louis Pasteur, F-67000 Strasbourg, France

Received May 22, 2001

The electronic structure, conformation, synthesis, and thermal decomposition pathways of the recently characterized dimolybdenum μ-nitrido complex $(AdS)_3Mo(\mu\text{-}N)Mo(N[^tBu]Ph)_3$ (**1exp**, Ad = adamantyl) are investigated by means of DFT calculations carried out on the model system $(HS)_3Mo(\mu\text{-}N)Mo(NH_2)_3$ (**1**). The observed asymmetry of the Mo(μ-N)Mo core is reproduced in the optimal conformation of **1** and assigned to the tendency for the electron density of the metal atoms to be preferably accommodated in the π orbitals of $Mo_{thiolate}$. The balance in the metal–ligand and ligand–ligand interactions conditioning the flow of the electron density along the Mo—(μ-N)—Mo framework, and eventually the relative activation of the molybdenum–nitrido bonds, appears very sensitive to the nature of the ancillary substituents on both the thiolate and the amido sides. On one hand, replacing HS by AdS in **1** increases the calculated value of $\Delta_{\mu-N-Mo}$ from 0.053 to 0.094 Å, close to the experimental value of 0.111 Å. The μ-nitrido complex with bulky thiolates **1a** is also less stable than **1** by 7.3 kcal·mol^{-1} with respect to its monometallic constituents. On the other hand, substituting the bulky N[^{t}Bu]Ph for NH_2 in the model complex **1b** induces an important charge transfer toward the thiolate moiety resulting in structural and energetic consequences of similar magnitude. Even though these substitutional effects are not likely to be fully additive in the real complex, both should contribute to an increase of the μ-N–$Mo_{thiolate}$ bond activation in **1exp**. The importance of this activation conditions the feasibility of the thermal decomposition of **1exp** promoted by benzonitrile which eventually yields the molybdenum thiolate dimer $(RS)_3Mo{\equiv}Mo(SR)_3$. The energy profile calculated for this reaction with model complex **1** in the presence of one or two molecules of acetonitrile shows that the axial fixation of the promoter on one or both molecular ends forms intermediates in which the μ-N—$Mo_{thiolate}$ bond is further activated with respect to the original complex. The consequence is an important, but still insufficient, decrease of the barrier to Mo—N bond breaking, from 53 to 37 kcal·mol^{-1}. Furthermore, the thermodynamic balance of the reaction leading from the acetonitrile adducts of **1** to $(HS)_3Mo{\equiv}Mo(SH)_3$ remains endothermic by 6.5 kcal·mol^{-1} for the monoadduct, and more for the diadduct. It therefore appears that bulky substituents on both ends of the dinuclear complex are essential to the completion of the reaction, from both the thermodynamic and the kinetic viewpoints.

1. Introduction

The development of efficient routes toward the fixation and the reductive cleavage of N_2 involving the formation of binuclear complexes of molybdenum,[1] niobium,[2] or vanadium[3] has provoked a surge of activity for understanding, by means of experiment[4] or theory,[5,6] the mechanism of these reactions. Efforts have also been made to expand the class of complexes susceptible to activate and break the NN bond in order to improve the selectivity and obtain better control

* Author to whom correspondence should be addressed. E-mail: benard@quantix.u-strasbg.fr.

(1) Laplaza, C. E.; Cummins, C. C. *Science* **1995**, *268*, 861.
(2) Zanotti-Gerossa, A.; Solari, E.; Giannini, L.; Floriani, C.; Chiesi-Villa, A.; Rizzoli, C. *J. Am. Chem. Soc.* **1998**, *120*, 437.
(3) Clentsmith, G. K. B.; Bates, V. M. E.; Hitchcock, P. B.; Cloke, F. G. N. *J. Am. Chem. Soc.* **1999**, *121*, 10144.
(4) Laplaza, C. E.; Johnson, M. J. A.; Peters, J. C.; Odom, A. L.; Kim, E.; Cummins, C. C.; George, G. N.; Pickering, I. J. *J. Am. Chem. Soc.* **1996**, *118*, 8623.
(5) Bates, V. M. E.; Clentsmith, G. K. B.; Cloke, F. G. N.; Green, J. C.; Jenkin, H. D. Ll. *Chem. Commun.* **2000**, 927.
(6) Cui, Q.; Musaev, D. G.; Svensson, M.; Sieber, S.; Morokuma, K. *J. Am. Chem. Soc.* **1995**, *117*, 12366.

10.1021/ic010543p CCC: $22.00
Published on Web 01/31/2002

of the reaction conditions. Concerning the *N-tert*-butylanilide complexes of Mo(III),[1,4] the possibility of replacing Mo−amido by Mo−thiolate linkages was found particularly attractive in this context, because the Mo−SR linkage is expected to be more stable than Mo−amido in the presence of Brønsted acids.[7] Only one example of a stable, well characterized, monomeric $Mo(SR)_3$ complex is known,[8] in probable relation with the tendency of the $Mo^{III}L_3$ fragment to dimerize into dinuclear complexes exhibiting a metal−metal triple bond.[9] The formation of these strongly bonded and stable dimeric complexes could, however, imply the transient existence of the monomeric species which could then be trapped into N_2 chemistry assuming favorable conditions. Starting from $N{\equiv}Mo(SAd)_3$ (Ad = 1-adamantyl), Cummins et al. recently reported the synthesis and characterization of the dimolybdenum μ-nitrido complex $(AdS)_3Mo(\mu\text{-}N)Mo(N[^tBu]Ph)_3$ (**1exp**).[7] At variance with the structure of the related (μ-nitrido)dimolybdenum hexakis(amide) complexes,[10] the Mo−N−Mo linkage in **1exp** is unsymmetrical. Similar μ-nitrido-bridged systems, either homo-[11,12] or heterobimetallic,[11,13] are believed to play important roles in metal-centered nitrogen atom transfer reactions and could be considered as the stable result of an incomplete nitrogen transfer.[10,14] In **1exp**, the Mo−N bond length is substantially longer on the tris(thiolate) fragment side, suggesting that this bond could be preferentially cleaved, thus completing the nitrogen transfer to yield the anticipated $Mo(AdS)_3$ fragment. The longest Mo−N bond was indeed broken by thermal decomposition in the presence of benzonitrile at room temperature, releasing species containing the $Mo(AdS)_3$ fragment and eventually yielding the molybdenum tris(thiolate) dimer $(AdS)_3Mo{\equiv}Mo(AdS)_3$.[2] The goal of the DFT calculations reported in the present work is to propose a mechanism and an energy profile for the fragmentation of the μ-nitrido complex and the dimerization of the molybdenum tris(thiolate), to specify the role of benzonitrile, and to characterize the transient species containing $Mo(AdS)_3$. The discussion concerning the electronic structure of **1exp** and the origin of the dissymmetry of the Mo−N−Mo core and its consequences concerning the relative strengths of the two molybdenum-nitrido bonds is also supported by extended Hückel (EHT) calculations.

2. Computational Details

In most calculations reported here, the bulky adamantyl and tertiobutyl substituents were replaced by hydrogens. The same model, $(HS)_3Mo(\mu\text{-}N)Mo(NH_2)_3$ (**1**, Figure 1), was used by Cummins et al. to carry out geometry optimizations on the μ-nitrido complex. However, the influence of the bulky substituents has been investigated by optimizing, with the same basis set, the geometries of two nitrido complexes closer to the real system, $(AdS)_3Mo(\mu\text{-}N)Mo(NH_2)_3$ (**1a**) and $(HS)_3Mo(\mu\text{-}N)Mo(N[^tBu]Ph)_3$ (**1b**), together with those of the mononuclear fragments $(AdS)_3Mo$ (**4a**) and $N{\equiv}Mo(N[^tBu]Ph)_3$ (**5b**). All calculations and geometry optimizations performed on model complexes **1**, **1a**, **1b**, **4a**, and **5b**, on the association products of complex **1** with one or two acetonitrile molecule(s), on all fragments resulting from the various possible dissociation pathways of **1**, and on the complexation of these framents with CH_3CN have been carried out using the formalism of the density functional theory (DFT) within the generalized gradient approximation (GGA), as implemented in the ADF program.[15] The formalism is based upon the local spin density approximation characterized by the electron gas exchange (Xα with $\alpha = {}^2/_3$) together with Vosko−Wilk−Nusair[16] parametrization for correlation. Nonlocal corrections due to Becke for the exchange energy[17] and to Perdew for the correlation energy[18] have been added. For first row atoms, the 1s shell was frozen and described by a single Slater function. The frozen core of heavier atoms, neon-like for S and krypton-like for Mo, was also modeled by a minimal Slater basis. For all nonmetal atoms, the Slater basis set used for the valence shell is of triple-ζ quality and supplemented with one polarization function.[19] The 4s and 4p shells of molybdenum are described by a double-ζ Slater basis; the 4d and 5s, by a triple-ζ basis, and the 5p shell is described by a single orbital. Relativistic corrections were not included. Complex **1exp** and its models, as well as fragments MoS_3H_3 (**4**), MoN_3H_6 (**2**), and their associations with acetonitrile are open-shell systems with a doublet ground state.

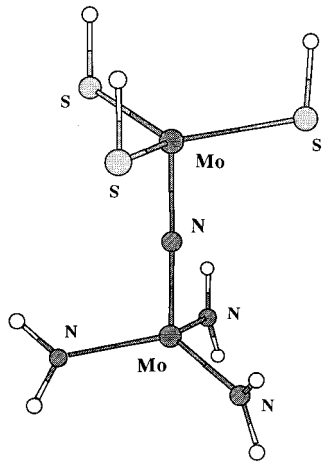

Figure 1. XMOL representation of the model complex $(HS)_3Mo(\mu\text{-}N)Mo(NH_2)_3$ (**1**), in the optimal structure obtained from DFT calculations.

(7) Agapie, T.; Odom, A. L.; Cummins, C. C. *Inorg. Chem.* **2000**, *39*, 174.
(8) Buyuktas, B. S.; Olmstead, M. M.; Power, P. P. *Chem. Commun.* **1998**, 1689.
(9) Cotton, F. A.; Walton, R. A *Multiple Bonds between Metal Atoms;* Oxford University Press: New York, 1993.
(10) Johnson, M. J. A.; Lee, P. M.; Odom, A. L.; Davis, W. M.; Cummins, C. C. *Angew. Chem., Int. Ed. Engl.* **1997**, *36*, 87.
(11) (a) Dehnicke, K.; Strähle, J. *Angew. Chem., Int. Ed. Engl.* **1981**, *20*, 413. (b) Dehnicke, K.; Strähle, J. *Angew. Chem., Int. Ed. Engl.* **1992**, *31*, 955. (c) Newton, C.; Edwards, K. D.; Ziller, J. W.; Doherty, N. M. *Inorg. Chem.* **1999**, *38*, 4032 and references therein.
(12) Bendix, J.; Weyhermüller, T.; Bill, E.; Wieghardt, K. *Angew. Chem., Int. Ed.* **1999**, *38*, 2766.
(13) Zheng, H.; Leung, W.-H.; Chim, J. L. C.; Lai, W.; Lam, C.-O.; Williams, I. D.; Wong, W.-T. *Inorg. Chim. Acta* **2000**, *306*, 184 and references therein.
(14) Tong, C.; Bottomley, L. A. *Inorg. Chem.* **1996**, *35*, 5108.
(15) (a) *ADF User's Guide, Release 1999;* Chemistry Department, Vrije Universiteit: Amsterdam, The Netherlands, 1999. (b) Baerends, E. J.; Ellis, D. E.; Ros, P. *Chem. Phys.* **1973**, *2*, 41. (c) te Velde, G.; Baerends, E. J. *J. Comput. Phys.* **1992**, *99*, 84. (d) Fonseca-Guerra, C.; Visser, O.; Snijders, J. G.; te Velde, G.; Baerends, E. J. *Methods and Techniques in Computational Chemistry: METECC-95*; Clementi, E., Corongiu, G., Eds.; STEF: Cagliari, Italy, 1995; pp 305−395.
(16) Vosko, S. H.; Wilk, L.; Nusair, M. *Can. J. Phys.* **1980**, *58*, 1200.
(17) (a) Becke, A. D. *J. Chem. Phys.* **1986**, *84*, 4524. (b) Becke, A. D. *Phys. Rev.* **1988**, *A38*, 3098.
(18) Perdew, J. P. *Phys. Rev.* **1986**, *B33*, 8882; **1986**, *B34*, 7406.
(19) (a) Snijders, J. G.; Baerends, E. J.; Vernooijs, P. *At. Data Nucl. Data Tables* **1982**, *26*, 483. (b) Vernooijs, P.; Snijders, J. G.; Baerends, E. J. *Slater type basis functions for the whole periodic system*; Internal Report Free University of Amsterdam: The Netherlands, 1981.

Calculations on these systems have therefore been carried out using the unrestricted formalism. Molecular bonding energies are reported with respect to an assembly of neutral atoms assumed isolated and in their ground state. The basis set superposition error (BSSE) has been estimated by the counterpoise method.[20] This means that single point calculations have been carried out on all fragments in their optimal geometry, taking advantage of the "ghost" orbital basis generated by the largest considered complex, that is, either $CH_3CN-(HS)_3Mo(\mu\text{-}N)Mo(NH_2)_3-NCCH_3$ or $CH_3CN-(HS)_3Mo{\equiv}Mo(HS)_3-NCCH_3$ for the dimerization part of the reaction. However, the BSSE corrections were found never to exceed 0.1 eV and were not taken into account in the reported results. The geometry optimization processes have been carried out by minimizing the energy gradient by the BFGS formalism[21] combined with a DIIS-type convergence acceleration method.[22] The optimization cycles were continued until all of the three following convergence criteria were fulfilled: (i) the difference in the *total energy* between two successive cycles is less than 0.001 hartree; (ii) the difference in the *norm of the gradient* between two successive cycles is less than 0.001 hartree·Å^{-1}; and (iii) the maximal difference in the *Cartesian coordinates* between two successive cycles is less than 0.01 Å.[23]

3. Structure and Bonding in 1 and in Related μ-Nitrido Complexes

Both the molybdenum (tris)thiolate and the molybdenum (tris)amido fragments are ML_3 moieties with approximate C_3 symmetry[24] and a formal d^3 population for each Mo(III) metal atom. In the isolated fragments, these electrons are accommodated in the set of t_{2g}-like metal orbitals.[25] The nature of the interactions with the equatorial ligands, however, introduces an important dissimilarity between the two sets of metal orbitals. The amido ligands are both σ and π donors. Both donation processes are effective through the metal e_g orbitals (mainly d_{xy} and $d_{x^2-y^2}$ combinations) while the t_{2g}-like orbitals retain a pure metal character. At variance with the $(NH_2)^-$ or $(NRR')^-$ ligands, the thiolate fragments display some acceptor character because of the dsp hybrids of sulfur. These high-energy ligand orbitals mainly interact with the metal π orbitals (d_{xz} and d_{yz}) which become lower in energy than their counterparts of the amide moiety. When both molybdenum fragments are connected through the nitrido bridge, they formally undergo a three-electron oxidation, which leaves only three d electrons in the metal framework. These electrons are shared between the two metal atoms via the Mo−N−Mo nonbonding pair of molecular orbitals with π character. If the two ML_3 fragments were identical, then these MOs would be antisymmetric and nonbonding with respect to the bridging nitrogen, leading to an equal share of the π density between metal atoms and to a strictly symmetric structure as represented in Scheme 1. This situation, with a possible deviation from 3-fold symmetry because of Jahn−Teller distortion, is encountered in the nitrido- and phosphido-bridged compounds characterized by Johnson et al. and linking two equivalent $Mo(NR_2)_3$ moieties.[10] Because of the distinct nature of the metal−ligand interactions in both moieties of **1**, the π orbitals of the thiolate moiety, stabilized by the back-donation interactions, are lower in energy than the pure metal orbitals of the amide fragment and tend to attract a larger share of the electron density. This leads to a pair of equivalent molecular orbitals similar to that pictured in Scheme 2 and which form the HOMO set of complexes **1**, **1a**, and **1b**, populated altogether with 3 electrons. The relative depopulation of Mo_{amide} makes the π donation from the bridging nitrogen more efficient in that direction and accounts for the origin of the structural dissymmetry along the Mo−N−Mo axis. The balance in the distribution of the metal π electron density, however, appears extremely sensitive to changes affecting either the orientation of the thiolate ligands or the donor strength of the amide ones. Because these factors are governed by the nature of the ancillary substituents grafted on the equatorial ligands, these substituents will have an important influence on the structure of the Mo−N−Mo framework and on the energetics of the process leading to Mo−N bond breaking.

Scheme 1

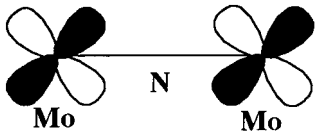

Scheme 2

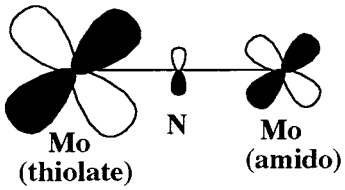

The orientation of the thiolate ligands, that is, the μ-N−Mo−S angle, can activate the μ-N−$Mo_{thiolate}$ bond through the nonbonding interaction between the thiolate lone pairs and the occupied π orbitals of N^{3-}. The thiolate lone pairs form a torus of high electron density below the plane of the three sulfur atoms, and its overlap with the orbitals of the bridging nitrogen is not negligible. It increases as the pyramidality of the $Mo(SR)_3$ fragment vanishes or becomes inverted because of steric crowding or axial coordination, and this interaction is unfavorable, both electronically and electrostatically. The system responds to the destabilizing interactions by a displacement of μ−N toward Mo_{amide}, which enhances the symmetry breaking of the Mo−N−Mo core. The shift of the bridging nitrogen away from $Mo_{thiolate}$ remains moderate as long as the $Mo(SR)_3$ fragment is pyramidalized opposite to μ-N, but the replacement of H by

(20) Boys, S. F.; Bernardi, F. *Mol. Phys.* **1970**, *19*, 553.
(21) Fisher, T. H.; Almlöf, J. *J. Phys. Chem.* **1992**, *96*, 9768.
(22) Versluis, L. Ph.D. Thesis, University of Calgary, Calgary, Alberta, Canada, 1989.
(23) The convergence criterion concerning the norm of the gradient has been tightened by a factor of 10 with respect to the default options of the program (0.01 hartree·Å^{-1}). In practice, with this restrictive condition, the energy difference in the two last iteration steps was of the order of 10^{-4} hartree, that is, ~0.06 kcal·mol^{-1}.
(24) In the tris-amido fragment, the amide planes are not strictly parallel to the molybdenum−nitrido axis. To reduce the repulsion between the nitrogen lone pairs, the H−N−H or the C−N−C planes deviate by ~20° from this axis. For model complex **1**, two conformations, with respective symmetries C_3 and C_{2v}, correspond to similar energies. In **1b**, the C_3 form more efficiently accommodates the bulky substituents.
(25) Albright, T. A.; Burdett, J. K.; Whangbo, M. H. *Orbital Interactions in Chemistry*; Wiley-Interscience: New York, 1985.

bulky substituents tends to flatten the MoS_3 group and, therefore, enhances the unfavorable interactions with μ-N. Geometry optimizations carried out at the DFT level illustrate this influence. In complex **1**, in which all bulky substituents are modeled by hydrogens, the difference $\Delta_{\mu-N-Mo}$ between the two μ-N−Mo bond lengths amounts to 0.053 Å only (Table 1). Replacing S−H ligands by the real S−Ad ligands in **1a** induces a significant stretching of the $N-Mo_{thiolate}$ bond, from 1.847 to 1.874 Å, and a consecutive shortening of the $N-Mo_{amide}$ bond (Table 1). The value of $\Delta_{\mu-N-Mo}$ in **1a**, 0.094 Å, becomes close to, but still lower than, the difference observed in the real complex **1exp**, 0.111 Å. The grafting of tertiobutyl and phenyl substituents on the amide groups enhances the donor ability of the ligands, and especially the π donor strength: EHT calculations show that the lone pair orbital energy of $(N[^tBu]Ph)^-$ is shifted up by more than 1 eV with respect to that of $(NH_2)^-$. As shown in Table 1, the donated density does not remain localized on Mo_{amide} but is shifted first toward the nitrido ligand, and then, via the partly occupied π frontier orbitals, toward the thiolate fragment. The main consequence is indeed a change in the relative polarities of the molecular moieties separated by the nitrido ligand: the thiolate fragment becomes negatively charged in **1b** (−0.10e) while it is undoubtedly positive in **1** and **1a** (+0.21e). Because this reorganization of the charge density is mainly concentrated on $Mo_{thiolate}$ whose positive charge decreases by 0.26e with respect to **1**, the interaction with μ-N becomes less favorable electronically and electrostatically, and the main structural consequence of the incorporation of bulky substituents to the amide moiety is again a stretching of the μ-N−$Mo_{thiolate}$ bond. The μ-N−$Mo_{thiolate}$ bond length calculated in **1b** is indeed 1.883 Å, compared to 1.847 Å in **1**. Because a similar activation of the μ-N−$Mo_{thiolate}$ bond can be induced for different reasons by the ancillary substituents either on the thiolate ligands or on the amide moiety, it is probable that both effects should be at least partly additive in the real complex **1exp**. This conjecture is supported by the experimental value of $\Delta_{\mu-N-Mo}$ being larger for **1exp** (0.111 Å) than for either **1a** (0.094 Å) or **1b** (0.075 Å) (Table 1).

4. Dissociation Pathways and Associated Fragments

Various pathways have been considered for the dissociation of the (μ-nitrido)dimolybdenum model complex **1**. Assuming first that the dissociation of **1** is not assisted by CH_3CN, two processes are possible in theory, depending on the Mo−N linkage that will be cleaved:

$$(HS)_3Mo(\mu\text{-}N)Mo(NH_2)_3\ (\mathbf{1}) \rightarrow Mo(NH_2)_3\ (\mathbf{2}) + N{\equiv}Mo(SH)_3\ (\mathbf{3}) \quad (1)$$

$$(HS)_3Mo(\mu\text{-}N)Mo(NH_2)_3\ (\mathbf{1}) \rightarrow Mo(SH)_3\ (\mathbf{4}) + N{\equiv}Mo(NH_2)_3\ (\mathbf{5}) \quad (2)$$

Assuming now that acetonitrile has been added to the solution, one should characterize first the adducts of CH_3CN to complex **1**. Two different monoadducts result from the fixation of CH_3CN either on the molybdenum supported by thiolate ligands or on the metal supported by amide ligands. A third possibility corresponds to the fixation of two acetonitrile molecules:

$$(HS)_3Mo(\mu\text{-}N)Mo(NH_2)_3\ (\mathbf{1}) + CH_3CN \rightarrow CH_3CN{-}(HS)_3Mo(\mu\text{-}N)Mo(NH_2)_3\ (\mathbf{1ac})_{th} \quad (3)$$

$$(HS)_3Mo(\mu\text{-}N)Mo(NH_2)_3\ (\mathbf{1}) + CH_3CN \rightarrow (HS)_3Mo(\mu\text{-}N)Mo(NH_2)_3{-}NCCH_3\ (\mathbf{1ac})_{am} \quad (4)$$

$$(HS)_3Mo(\mu\text{-}N)Mo(NH_2)_3 + 2CH_3CN \rightarrow CH_3CN{-}(HS)_3Mo(\mu\text{-}N)Mo(NH_2)_3{-}NCCH_3\ (\mathbf{1ac})_2 \quad (5)$$

For each of these possibilities, different modes of fixation could be envisioned for acetonitrile, namely (i) an approach along the molecular axis, eventually leading to an axial, η^1 ligation and to a trigonal bipyramid coordination for the considered metal(s) (Scheme 3, right); and (ii) an approach and a coordination along the equatorial plane, yielding an approximate square pyramid conformation and an η^1 coordination mode for the acetonitrile adduct (Scheme 4, left). Variants of the latter case might lead to η^2 coordination modes in which acetonitrile could be either coplanar with the average equatorial plane (Scheme 4, right) or perpendicular to it (Scheme 4, center).

As for the naked complex **1**, each of the acetonitrile adducts could in principle dissociate along pathways similar to pathway 1 or 2 involving the breaking of one Mo−N bond. Because the Mo−N bond close to the amide ligands is shortest in **1** and less liable to be broken in the unperturbed complex, the cleavage of this bond was only considered after an activation induced by the axial complexation of Mo_{amide} by CH_3CN, yielding $(\mathbf{1ac})_{am}$:

$$(HS)_3Mo(\mu\text{-}N)Mo(NH_2)_3{-}NCCH_3\ (\mathbf{1ac})_{am} \rightarrow Mo(NH_2)_3{-}NCCH_3\ (\mathbf{2ac}) + N{\equiv}Mo(SH)_3\ (\mathbf{3}) \quad (6)$$

The cleavage of the longest Mo−N bond, further activated by the coordination of acetonitrile on the thiolate side, was therefore the only process investigated when starting from either $(\mathbf{1ac})_{th}$ or $(\mathbf{1ac})_2$:

$$CH_3CN{-}(HS)_3Mo(\mu\text{-}N)Mo(NH_2)_3\ (\mathbf{1ac})_{th} \rightarrow CH_3CN{-}Mo(SH)_3\ (\mathbf{4ac}) + N{\equiv}Mo(NH_2)_3\ (\mathbf{5}) \quad (7)$$

$$(\mathbf{1ac})_2 \rightarrow Mo(SH)_3{-}NCCH_3\ (\mathbf{4ac}) + N{\equiv}Mo(NH_2)_3\ (\mathbf{5}) + CH_3CN \quad (8)$$

The geometry of complex $(\mathbf{1ac})_{th}$ was optimized assuming either the axial or the equatorial η^1 and η^2 coordination modes of CH_3CN. The side-on conformations were found dissociative, and the equatorial, end-on isomer, is higher in energy than the axial form (Figure 3). This isomer leads to dissociation products in a high-energy conformation and is not expected to take part in process 7. The axial conformation of $(\mathbf{1ac})_{th}$ was therefore assumed to study the dissociation process. Reactions 7 and 8 yield the mononuclear tris(thiolate) fragment **4ac** complexed with one acetonitrile molecule. By identifying this complex with the "species

Table 1. Selected Structural Parameters and Mulliken Charges Calculated for the Dimolybdenum μ-Nitrido Model Complexes **1**, **1a**, and **1b**, Molybdenum (Tris)thiolate Dimer **6**, Their Fragments[a], and Various Systems Resulting from Their Association with One or Two Molecules of Acetonitrile (acetyl)[b]

	1	**1a**	**1b**	**1exp**	**1(acet)** thiolate	**1(acet)** amide	**1(acet)$_2$**	**2**	**2(acet)**	**3**	**4**	**4(acet)**	**5**	**5b**	**6**
							Structural Parameters								
μ(N)−Mo$_{thiolate}$	1.847	1.874	1.883	1.882	1.986	1.800	1.889			1.667					
μ(N)−Mo$_{amide}$	1.794	1.780	1.808	1.771	1.732	1.869	1.805						1.671	1.676	
S−Mo$_{thiolate}$	2.345	2.345	2.350	2.308	2.362	2.348	2.366			2.354	2.319	2.344			2.343
N−Mo$_{amide}$	1.981	1.984	2.036	1.977	1.983	1.996	1.992	1.986	1.994				1.990	2.040	
Mo−Mo															2.247
N$_{acet}$−Mo$_{thiolate}$					2.142		2.229					1.972			
N$_{acet}$−Mo$_{amide}$						2.248	2.335		1.955						
μ(N)−Mo−S [c]	98.6	94.0	103.8	93.7	90.1	99.6	91.6			101.6		84.2*			
μ(N)−Mo−N [c]	101.1	101.8	102.9	105.9	101.9	94.9	96.8		82.5*				104.6	102.0	
Mo−S−X [d]	97.5	115.4	96.6	115.5	101.4	96.7	100.3			94.6	98.8	102.2			93.7
Mo−N−H [e]	124.4	124.0	131.7	133.8	124.0	123.9	123.2	125.3	126.3				124.4	129.9	
							Charges								
Mo$_{thiolate}$	+0.86	+0.63	+0.60		+0.97	+0.89	+1.00			+0.78	+0.57	+0.81			+0.36
Mo$_{amide}$	+1.87	+1.88	+1.89		+1.94	+2.00	+2.04	+1.37	+1.71				+1.71	+1.78	
N$_{nitrido}$	−0.82	−0.83	−0.89		−0.83	−0.83	−0.88			−0.40			−0.52	−0.64	
N$_{amide}$	−0.43	−0.44	−0.72		−0.44	−0.42	−0.42	−0.47	−0.46				−0.43	−0.72	
amide moiety	+0.61	+0.62	+0.99		+0.68	+0.68	+0.72	0.0	+0.27				+0.52	+0.64	
S$_{thiolate}$	−0.13	−0.15	−0.11		−0.15	−0.13	−0.15			−0.06	−0.13	−0.16			−0.04
thiolate moiety	+0.21	+0.21	−0.10		+0.22	+0.26	+0.25			+0.40	0.0	+0.12			0.0
bond energies [f]	−97.053	−517.009	−491.868		133.974	−133.821	−170.533	−53.742	−91.153	−40.670	−30.428	−68.032	−64.321	−459.515	−66.016

[a] **1** = (SH)$_3$Mo(μ-N)Mo(NH$_2$)$_3$; **1a** = (SAd)$_3$Mo(μ-N)Mo(NH$_2$)$_3$; **1b** = (SH)$_3$Mo(μ-N)Mo(N[^{t}Bu]Ph)$_3$; **1exp** = (SAd)$_3$Mo(μ-N)Mo(N[^{t}Bu]Ph)$_3$; **2** = Mo(NH$_2$)$_3$; **3** = N≡Mo(SH)$_3$; **4** = Mo(SH)$_3$; **5** = N≡Mo(NH$_2$)$_3$; **5b** = N≡Mo(N[^{t}Bu]Ph)$_3$; **6** = (SH)$_3$Mo≡Mo(SH)$_3$. [b] Structural parameters observed for the dimolybdenum complex **1exp** are displayed. Distances are in Å, angles in deg, charges in e, and energies in eV. [c] In fragments **2**(acet) and **4**(acet), μ-N represents an atom positioned at infinity on the 3-fold symmetry axis in the direction opposite to N$_{acet}$. The angular values referring to this dummy atom are starred. [d] X = H (**1** and **1b**) or C (**1a**). [e] X = H (**1** and **1a**) or C (**1b**). X is closest to the nitrido nitrogen. [f] Optimal bond energies have also be obtained for CH$_3$CN (−36.183 eV), CH$_3$CN···(NH$_2$)$_3$Mo≡N (−100.646 eV), Mo(SAd)$_3$ (−450.704 eV), and CH$_3$CN···(SH)$_3$Mo≡Mo(SH)$_3$···NCCH$_3$ (−138.611 eV).

Scheme 3

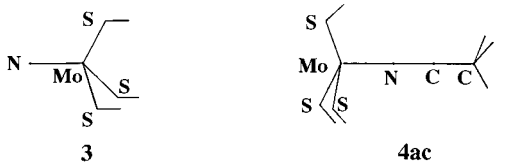

3 **4ac**

Scheme 4

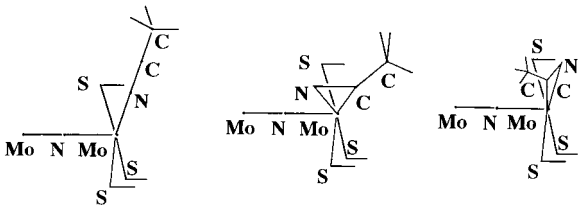

containing the molybdenum tris(thiolate) fragment" which appears as a transient intermediate in the reaction reported by Cummins, it should be possible to dimerize it into the triply bonded dimetal compound $(HS)_3Mo{\equiv}Mo(SH)_3$:

$$2Mo(SH)_3{-}NCCH_3\ (\mathbf{4ac}) \rightarrow (HS)_3Mo{\equiv}Mo(SH)_3\ (\mathbf{6}) + 2CH_3CN \quad (9)$$

The two acetonitrile molecules can be either released or kept loosely attached in the coordination sphere of the metal atoms. Calculations suggest that such weak associations in axial position between complexes **5** or **6** and acetonitrile might contribute to make reaction 9 slightly easier both thermodynamically and kinetically.

5. Energy Profiles

5.1 Formation of 1 and Coordination of Acetonitrile. The energetic profiles calculated for reactions 1−9 are summarized in Figure 2, and the corresponding fragment energies are reported in Table 1. Assuming first the dissociation, or the formation, of **1** not to be assisted by acetonitrile, the energy of fragments **2** and **3** was found to be 61 kcal·mol^{-1} in excess of that of the (μ-nitrido) complex. The strongly exothermic process corresponding to the inverse of reaction 1 represents in fact the route that was followed to synthesize complex **1exp**. As expected from the relative lengths and from the assumed strengths of the two molybdenum−nitride bonds, the decomposition of **1** into the molybdenum (tris)thiolate and the nitrido (tris)amide fragments (reaction 2) is somewhat easier than process 1. The activation energy (53 kcal·mol^{-1}) however remains very high, and this should explain why a clean decomposition process along reaction path 2 could not be observed at room temperature.[7] According to the operation mode described by Agapie, Odom, and Cummins, such a clean thermal decomposition, eventually leading to $N{\equiv}Mo(NR)_3$, and to the molybdenum (tris)thiolate dimer, was only obtained when adding benzonitrile, either in excess or in a substoichiometric amount, to a toluene solution of **1exp** at room temperature.[7] To investigate the role of the cyanide group in the decomposition process, acetonitrile was coordinated to molybdenum in **1** either on the thiolate side (reaction 3) or on the amide side (reaction 4), or on both metal atoms (reaction 5). The influence of the coordination mode on the structure and on the energy of the acetonitrile monoadduct was investigated in some detail for $(\mathbf{1ac})_{th}$. Both types of η^2 coordination (Scheme 4) were found to be dissociative. Only the η^1 coordination mode, either axial or equatorial, leads to stable minima (Figure 3). The acetonitrile fixation is stabilized by 17.0 kcal·mol^{-1} in the axial form and by 9.2 kcal·mol^{-1} in the equatorial, square pyramid conformation (Figure 3). It seems, however, that the latter form represents a dead end as far as the Mo−N bond breaking is concerned, because the dissociation of the equatorial monoadduct yields a very high energy isomer of **4**(acet) (+36 kcal·mol^{-1}) with approximate square planar conformation. We will, therefore, refer to the axial, η^1 conformation of $(\mathbf{1ac})_{th}$ as the only isomer that could be involved in the dissociation process.

The axial fixation of CH_3CN on the amide moiety yields another monoadduct, $(\mathbf{1ac})_{am}$, stabilized by 13.5 kcal·mol^{-1}, instead of 17 kcal·mol^{-1} for $(\mathbf{1ac})_{th}$. The coordination of two CH_3CN molecules further stabilizes the complex, but the energy balance in $(\mathbf{1ac})_2$ with respect to **1** (−26 kcal·mol^{-1}) is less favorable than the stabilization resulting from the single-site coordination of two CH_3CN molecules on separate molecules of **1**, either both on the (tris)thiolate side (−34 kcal·mol^{-1}) or on opposite sides (−30.5 kcal·mol^{-1}) (Figure 2). The geometries optimized for $(\mathbf{1ac})_{th}$, $(\mathbf{1ac})_{am}$, and $(\mathbf{1ac})_2$ (Table 1) allow us to readily interpret the relative values of these stabilization energies in terms of the trans effect. The shortest and strongest single association of **1** with acetonitrile ($Mo_{thiolate}{-}N_{acet}$ = 2.14 Å) occurs on the (tris)thiolate moiety. The coordination of CH_3CN further activates the longest μ-N−Mo bond, whose length increases from 1.85 to 1.99 Å. Note that the conformation of MoS_3 has become nearly planar, which enhances the unfavorable four-electron interactions between S and μ-N and contributes to the stretching of the μ-N−$Mo_{thiolate}$ bond. The weakening of the μ-N−$Mo_{thiolate}$ bond induces a contraction of the opposite μ-N−Mo_{amide} bond, from 1.79 to 1.73 Å. The approach of one acetonitrile molecule on the Mo_{amide} side results in a weaker complexation ($Mo_{amide}{-}N_{acet}$ = 2.25 Å) and to a lower stabilization energy but leads to an inversion of the two μ-N−Mo distances. In $(\mathbf{1ac})_{am}$, the most activated μ-N−Mo bond (1.87 Å) belongs to the amide moiety, whereas the opposite μ-N−$Mo_{thiolate}$ distance is shortened to 1.80 Å (Table 1). As $\Delta_{\mu-N-Mo}$ significantly increases with substituted equatorial ligands, the inversion of the μ-N−Mo distances could be less dramatic, if occurring at all, in the Mo_{amide}−cyanide monoadducts derived from complexes **1a**, **1b**, and principally **1exp**. The trend is expected, however, to be similar. In the dicyanide complex $(\mathbf{1ac})_2$, the presence of two CH_3CN molecules opposite to each other at the axial ends of the complex inhibits the propagation of the trans effect along the molecular axis. As a consequence, the coordination of the CH_3CN molecules is weaker than in either monoadduct ($N{-}Mo_{thiolate}$ = 2.23 Å; $N{-}Mo_{amide}$ = 2.33 Å), and both μ-N−Mo distances are slightly activated. As expected, the μ-N−$Mo_{thiolate}$ bond is more sensitive to the axial coordination of CH_3CN because of the reduced

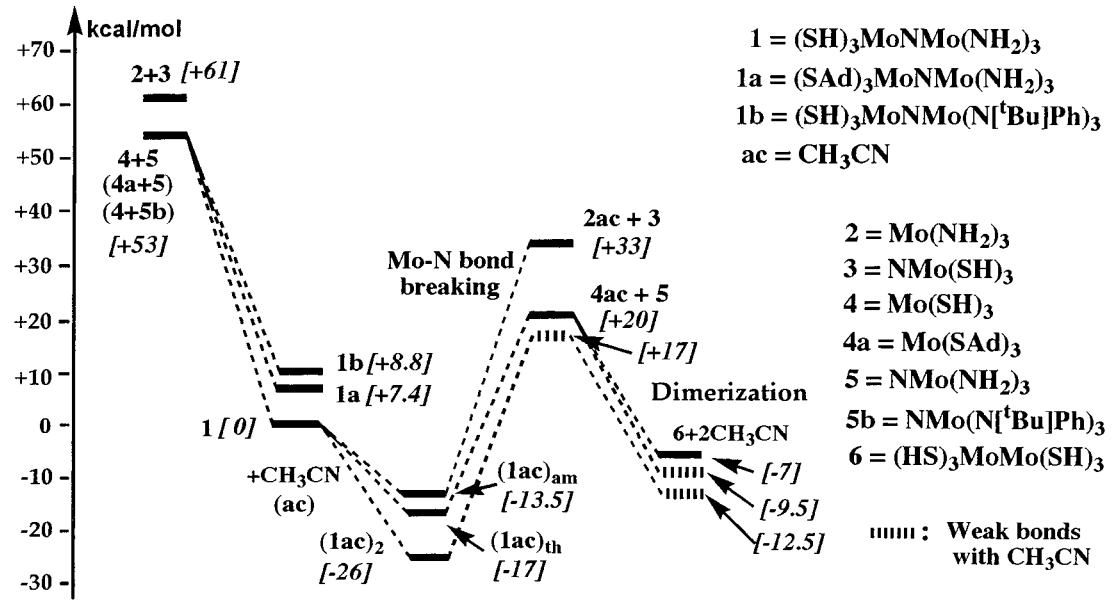

Figure 2. Calculated energy profile corresponding to the formation of the dimolybdenum model complexes **1**, **1a**, and **1b** from the monometallic fragments and to the thermal decomposition of **1** promoted by acetonitrile and leading to the (tris)thiolate dimer **6**.

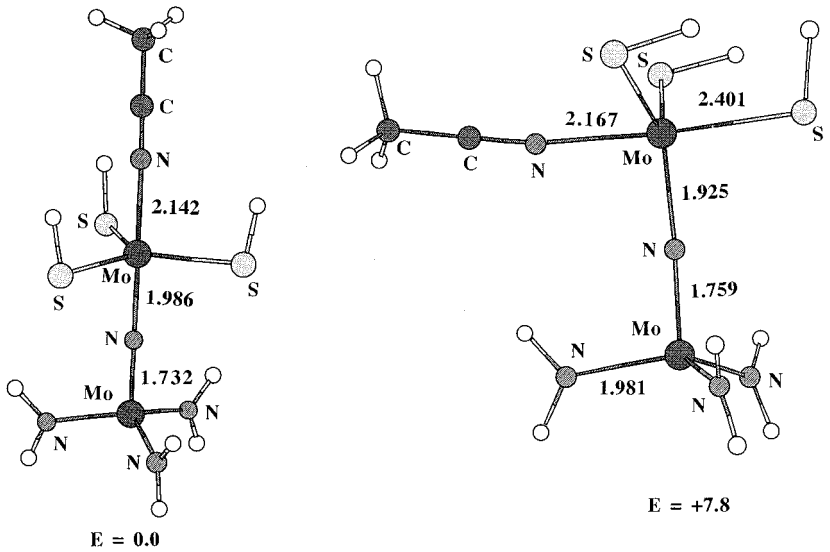

Figure 3. Optimized structures and relative energies (kcal·mol^{-1}) of the two stable isomers of the acetonitrile monoadduct obtained from an axial or from an equatorial approach of CH_3CN to $Mo_{thiolate}$ in **1**.

pyramidality at $Mo_{thiolate}$ and $\Delta_{\mu-N-Mo}$ eventually increases from 0.053 to 0.084 Å (Table 1).

5.2 Decomposition Pathways of the Acetonitrile Adducts. The preceding discussion of the geometry of the three acetonitrile adducts already provides a hint about the decomposition pathway preferred by model complex **1**: the less endothermic route should involve the adduct displaying the most activated μ-N−Mo bond, namely the monoadduct on $Mo_{thiolate}$ (**1ac**)$_{th}$. According to reaction 7, the cleavage of the activated μ-N−$Mo_{thiolate}$ bond leads to the fragments $Mo(SH)_3$−$NCCH_3$ (**4ac**) and N≡$Mo(NH_2)_3$ (**5**). The energy requested to complete this cleavage amounts to 37 kcal·mol^{-1}, to be compared with the 53 kcal·mol^{-1} necessary to break the same μ-N−$Mo_{thiolate}$ bond in the absence of acetonitrile (Figure 2). In fragment **4ac**, the acetonitrile ligand is strongly attached to molybdenum (Mo−N = 1.972 Å), inducing a slight elongation (0.025 Å) of the Mo−S bonds with respect to $Mo(SH)_3$. Furthermore, the strong attachment of CH_3CN has induced a large opening of the thiolate ligand umbrella and an inversion of the pyramidality at $Mo_{thiolate}$ (Table 1, Scheme 3).

The value of 37 kcal·mol^{-1} calculated for the activation energy, however, remains too high to account for the spontaneous dissociation of **1exp** observed at room temperature. It is important to note that the substitutions of S_3H_3 by S_3Ad_3 and of $(NH_2)_3$ by $(N[^tBu]Ph)_3$ will both contribute to further activate the μ-N−$Mo_{thiolate}$ bond and to lower the energy barrier. The bulky substituents at both molecular ends were shown to reduce the relative stability of the μ-nitrido complex with respect to the mononuclear species and to make still easier the μ-N−$Mo_{thiolate}$ bond cleavage. This activation of the binuclear complex with respect to its monometallic fragments was calculated to be 7.4 kcal·mol^{-1} for **1a**, and 8.8 kcal·mol^{-1} for **1b** (Figure 2). The effects induced at each

molecular end are expected to be at least partly additive. This upward energy shift should be transmitted to the acetonitrile adducts. It is also expected that the sterically crowded ligand restricts the accessibility of $Mo_{thiolate}$ to the cyanide promoter, which will destabilize further the $(\mathbf{1ac})_{th}$ intermediate. Then, the cleavage of the μ-N−Mo bond is concerted with (i) the opening of the $(SAd)_3$ ligand umbrella (Scheme 3), which enhances the destabilizing interactions between S and μ-N, and (ii) the strengthening of the coordination with the cyanide ligand.

If the thermal cleavage could be initiated from the monoadduct of CH_3CN on Mo_{amide}, a hypothesis which appears unlikely with model system **1** because $(\mathbf{1ac})_{am}$ is significantly less stable than $(\mathbf{1ac})_{th}$ (Figure 2), the μ-N−Mo bond in a position to be broken would in such a case be the μ-N−Mo_{amide} bond, which has become the most activated one as a consequence of the propagation of the trans effect (reaction 6). The energy requested to achieve the reaction, however, remains high (46.5 kcal·mol^{-1} with model **1**) with respect to that of the converse process 7 leading to the (tris)-thiolate species.

If monoadduct $(\mathbf{1ac})_{th}$ is likely to be the reactant when the cyanide promoter is added in substoichiometric amounts, the use of the same adjunct in large excess should yield the more stable dicyanide complex $(\mathbf{1ac})_2$ (Figure 2). As noted above, the activation of the μ-N−$Mo_{thiolate}$ bond in $(\mathbf{1ac})_2$ is hardly greater than in unsubstituted complex **1**, and the reduction of the energy barrier with respect to unpromoted reaction *2* mainly results from the strong coordination of CH_3CN to the monomeric (tris)thiolate fragment. When the cleavage reaction is completed, the second acetonitrile molecule is only loosely attached to the $N{\equiv}MoN_3H_6$ fragment because of the very strong trans effect induced by the nitrido ligand. A Mo−$N_{cyanide}$ equilibrium distance of 2.83 Å was found from direct geometry optimization of $N{\equiv}MoN_3H_6{-}NCCH_3$, and the associated stabilization energy amounts to 3.2 kcal·mol^{-1}. To summarize, the energy barrier associated with the dissociation of $(\mathbf{1ac})_2$ into $CH_3CN{-}Mo(SH)_3$ and $N{\equiv}MoN_3H_6$ loosely associated with an acetonitrile molecule, according to reaction 8, is 43 kcal·mol^{-1}, instead of 37 kcal·mol^{-1} for the similar cleavage reaction carried out from the most stable cyanide monoadduct. One should predict from these results the cleavage reaction of **1** to be significantly easier when using strictly stoichiometric or substoichiometric amounts of the cyanide promoter. In fact, the results obtained with **1exp** lead to a rather different interpretation: the dimerization of the (tris)-thiolate fragment seems to be faster, and the ratio of $N{\equiv}Mo(N[^tBu]Ph)_3$ to $(AdS)_3Mo{\equiv}Mo(SAd)_3$, closer to that of a stoichiometric reaction when benzonitrile is used in excess.[7] We, therefore, suspect that the bulky adamantane substituents reduce the accessibility of $Mo_{thiolate}$ to benzonitrile, so that the monoadduct on Mo_{amide} becomes predominant and leads to uncontrolled decomposition processes when benzonitrile is added in substoichiometric quantities to a solution of **1exp**.

5.3 Dimerization of the (Tris)thiolate Fragment. We have considered the formation of the tris(thiolate) dimer **6** from the condensation of two molecules of $CH_3CNMoS_3H_3$ (**4ac**) (reaction 9). This mononuclear complex has been obtained from the thermal cleavage of the activated μ-N−Mo bond either in $(\mathbf{1ac})_{th}$ or in $(\mathbf{1ac})_2$. The dimerization energy profile represented in Figure 2 refers to a single molecule of **4ac**, which means that the energy released in the formation of one molecule of dimer is twice as much, namely 59 kcal·mol^{-1}. The formation of a triple bond between molybdenum atoms generates a strong trans effect which considerably attenuates the strength of axial coordination, as observed in most compounds with a multiple Mo−Mo bond.[9] Weak associations between dimer **6** and two molecules of acetonitrile (d_{Mo-N} = 3.21 Å) are, however, obtained from the calculations and contribute ∼5.5 kcal·mol^{-1} to the overall stability of the dimer.

It is important to note that the dimerization reaction observed by Agapie et al. *starting from complex **1exp*** could probably not be observed with model complex **1**. Figure 2 shows that the energetic balance of the dimerization reaction, even considering the weak axial interactions, is *endothermic* with respect either to the CH_3CN monoadduct on $Mo_{thiolate}$ (by 7.5 kcal·mol^{-1}), or, still more conspicuously, to the dicyanide complex $(\mathbf{1ac})_2$. These cyanide intermediates should be made less stable for the reaction to proceed toward the molybdenum (tris)thiolate dimer. The presence of bulky ligands *on the two metals* should contribute to reduce by as much as 10−15 kcal·mol^{-1}, according to the amount of additivity in the influence of ancillary substituents, the relative stability of the μ-nitrido dinuclear complex with respect to its decomposition fragments. This activation should be still enhanced in the mono- and dicyanide intermediates by weakening the axial Mo−NCR bonds due to steric contacts. Reducing the stability of the mono- and dicyanide intermediates will make the dimerization reaction thermodynamically possible and also kinetically easier by decreasing the energy barrier associated with the formation of the mononuclear (tris)thiolate species $CH_3CNMoS_3R_3$.

6. Summary and Conclusion

Modeling the energy profiles associated with various pathways for the thermal decomposition of $S_3H_3Mo(\mu\text{-}N)\text{-}MoN_3H_6$ provides hints to explain the mechanism of the μ-N−$Mo_{thiolate}$ bond cleavage observed with complex **1exp** in the presence of benzonitrile. The asymmetry of the Mo−N−Mo core in the μ-nitrido complex **1exp** and its model is interpreted as a consequence of the different interactions that develop between the equatorial ligands and the metal π orbitals in the thiolate and in the amide moieties. The relative stabilization of the π orbitals in $Mo_{thiolate}$ provides these orbitals with a larger share of the d valence electrons, which impedes the μ-N → $Mo_{thiolate}$ π donation and yields a longer Mo−N bond. Metal−ligand and ligand−ligand interactions involving both types of equatorial surroundings were shown to strongly influence the structure of the Mo−N−Mo framework and to be sensitive to the effects of ancillary substituents on the thiolate and on the amide moieties. The presence of bulky ligands on both molecular ends contributes to enhance the activation of the

μ-N−$Mo_{thiolate}$ bond. A brute force cleavage of this bond, however, remains a high energy process (53 kcal·mol^{-1} from **1**, 46 kcal·mol^{-1} from **1a**, 44 kcal·mol^{-1} from **1b**, probably less from **1exp**). Adding acetonitrile or benzonitrile will yield intermediates in which one or two cyanide molecules weakly coordinate to the metal atoms of the μ-nitrido complex. The relative stabilities of these intermediates depend on the pyramidality at $Mo_{thiolate}$ and also probably on the axial accessibility of the metal atoms. Both factors are monitored by the nature of the thiolate substituents. A tuning of the π donor ability of the amide ligands, also governed by the substituents, equally contributes to activate the μ-N−$Mo_{thiolate}$ bond. The cleavage of this bond from the cyanide intermediates then requires a much reduced energy barrier due to the combination of two effects: (i) an increased activation of the μ-N−$Mo_{thiolate}$ bond either in the RCN monoadduct on $Mo_{thiolate}$ or in the diadduct and (ii) an important stabilization of the monomeric Mo (tris)thiolate fragment due to a stronger coordination of RCN. The thermodynamic achievability of the reaction is then conditioned by the amount of energy recovered from the dimerization of $Mo(SR)_3$ and the concurrent detachment of the cyanide ligands.

If the salient features of the reaction pathways displayed in Figure 2 are likely to be general, the thermodynamic balance of the reaction appears to be delicate, and its successful achievement might eventually be conditioned by electronic and steric factors related to the nature of the equatorial ligands. Calculations carried out on system **1** in which all ancillary substituents are modeled by hydrogens conclude that the dimerization of the molybdenum (tris)-thiolate complex is an endothermic process. It was, however, evidenced that (i) the flattening of the MoS_3 pyramid induced by bulky substituents such as adamantane enhances the S $\leftrightarrow$ μ-N repulsion and that (ii) the enhanced π donation induced by the combined acyl and aryl substitution on the amide ligands initiates a charge transfer toward the thiolate moiety. Both effects contribute to activate the μ-N−$Mo_{thiolate}$ bond. A greater bond activation decreases the relative stability of the dimolybdenum μ-nitrido complex and displaces the thermodynamic balance of the system toward the formation of the Mo (tris)thiolate dimer.

After this article had been accepted for publication, we became aware of the very recent work by Solari et al. reporting the four-electron reduction of the N≡N bond leading to the dinuclear complex $[(Mes)_3Mo{=}N{-}N{=}Mo(Mes)_3]$ (Mes = 2,4,6-$Me_3C_6H_2$), followed by the cleavage of the central N−N bond.[26] In the process reported by Solari, the N−N bond cleavage is not thermal but photoinduced and yields the symmetric, μ-nitrido complex $[(Mes)_3Mo{-}N{-}Mo(Mes)_3]$.

Acknowledgment. Calculations have been carried out in part at the Centre Universitaire et Régional de Ressources Informatiques (CURRI, Université Louis Pasteur, Strasbourg, France) and in part at the IDRIS computer center (CNRS, Orsay, France). We are pleased to thank Prof. C. C. Cummins for expressing his sympathy and encouragement, and we thank a reviewer for helpful suggestions.

Supporting Information Available: Tables of Cartesian coordinates, Mulliken atomic net charges, and atomic spin densities (for the systems with a doublet ground state) at the optimal geometry for **1**, **1a**, **1b**, CH_3CN (**ac**), **1**(**ac**)$_{th}$, **1**(**ac**)$_{am}$, **1**(**ac**)$_2$, **2**, **2ac**, **3**, **4**, **4a**, **4**(**ac**), **5**, **5b**, **5ac**, **6**, **6**(**ac**)$_2$.This material is available free of charge via the Internet at http://pubs.acs.org.

IC010543P

(26) Solari, E.; Da Silva, C.; Iacono, B.; Hesschenbrouck, J.; Rizzoli, C.; Scopelliti, R.; Floriani, C. *Angew. Chem., Int. Ed.* **2001**, *40*, 3907.